THE JOURNAL OF BIOLOGICAL CHEMISTRY
Vol. 277, No. 1, Issue of January 4, pp. 686–693, 2002
Printed in U.S.A.

The Angiopoietin-like Factor Cornea-derived Transcript 6 Is a Putative Morphogen for Human Cornea*

Received for publication, June 21, 2001, and in revised form, October 22, 2001
Published, JBC Papers in Press, October 26, 2001, DOI 10.1074/jbc.M105746200

Ron Peek‡§, Richard A. Kammerer¶, Sabine Frank¶, Irene Otte-Höller‖, and Johan R. Westphal‖

From the ‡Department of Molecular Immunology, Netherlands Ophthalmic Research Institute, Amsterdam 1105 BA, The Netherlands, the ¶Department of Biophysical Chemistry, Biozentrum, University of Basel, Basel CH-4056, Switzerland, and the ‖Department of Pathology, University Medical Center, Nijmegen 6500 HB, The Netherlands

The human cornea-specific protein cornea-derived transcript 6 (CDT6) is a member of the angiopoietin gene family. We report the structural and functional characterization of CDT6. We demonstrate that CDT6 is a secreted protein that folds into disulfide-linked homotetramers by coiled-coil interactions. The finding that CDT6 is expressed at high levels in the avascular corneal stromal layer suggested that the protein, similar to certain angiopoietins, acts as a negative regulator of angiogenesis. To test this hypothesis and to assay the effect of the protein on a growing tissue with high vascular density, CDT6 was expressed in a mouse xenograft model. Expression of CDT6 led to a reduction in tumor growth and aberrant blood vessel formation by inducing massive fibrosis. Interestingly, expression of CDT6 also resulted in the deposition of extracellular matrix components typical for the mature corneal stromal layer. These observations strongly suggest a role as morphogen for CDT6 in inducing a corneal phenotype *in vivo*.

The human cornea possesses several unique characteristics such as resistance to neoplasia, light refraction, optical transparency, and avascularity. Three separated cellular components can be distinguished as follows: the epithelium, the stroma, and the endothelium. The epithelium consists of several cell layers that are constantly replaced by proliferation and differentiation of the corneal limbal stem cells. The stromal layer constitutes about 90% of corneal thickness and is produced by the embedded fibroblast-like keratocytes. This layer consists of a highly specialized extracellular matrix largely composed of specific collagen fibrils surrounded by proteoglycans to produce a strong and transparent lattice. The inner cellular layer, the endothelium, consists of a single layer of hexagonal cells and regulates corneal osmotic balance (1). As the unique properties of the human cornea are likely to be reflected in the gene expression pattern of this tissue, several studies have been focused on the characterization of gene products contributing to corneal development and integrity (2–4). By differential hybridization of a human adult corneal cDNA library, we recently have identified a novel cornea-specific gene product named cornea-derived transcript 6 (CDT6)[1] (4). Data base similarity searches revealed that CDT6 is homologous to the gene family of the angiopoietins. These glycoproteins signal vascular morphogenesis and maintenance by binding to the vascular endothelial Tie2 receptor (5–7). Angiopoietins are characterized by three domains as follows: a signal sequence for protein secretion, a coiled-coil domain that mediates multimerization, and a fibrinogen-like domain that binds the Tie2 receptor. Although CDT6 shares all these features with the angiopoietins, it does not bind the Tie2 receptor. This indicated that CDT6 does not function as a "true" angiopoietin (7). However, the finding that CDT6 is expressed in a tissue, which is normally devoid of blood vessels, suggested that the protein, similar to angiopoietin-1 and angiopoietin-2, acts as a negative regulator of angiogenesis. This suggestion is supported by the finding that expression of CDT6 is restricted to the corneal stromal layer, the site of pathologic angiogenesis.

In this report we describe the structural and functional characterization of CDT6. Our results demonstrate that CDT6 is a secretory protein that forms disulfide-linked tetramers. Expression of CDT6 in a mouse xenograft model was used to assay the effect of this protein in a growing tissue with high vascular density. Expression of CDT6 led to a reduction in tumor growth and aberrant blood vessel formation by inducing massive fibrosis. Interestingly, expression of CDT6 also resulted in the deposition of extracellular matrix components typical for the mature corneal stromal layer. These observations strongly suggest a role as morphogen for CDT6 in inducing a corneal phenotype *in vivo*.

EXPERIMENTAL PROCEDURES

Production of Recombinant CDT6cc—A DNA fragment coding for the coiled-coil domain of CDT6 (CDT6cc; residues Glu-47 to Gln-122) was amplified by PCR and ligated into the *Bam*HI/*Eco*RI site of the bacterial expression vector pPEP-T (8). Recombinant insert DNA was verified by DNA sequencing.

Production and purification of CDT6cc were carried out as described (8). The protein contains two additional residues, Gly and Ser, at its N terminus. The recombinant polypeptide chain fragment was analyzed in 5 mM sodium phosphate buffer (pH 7.4) supplemented with 150 mM sodium chloride. The concentration of CDT6cc was determined by Trp and Tyr absorption in 6 M guanidine hydrochloride (9).

Biophysical Characterization of CDT6cc—CD spectroscopy and analytical ultracentrifugation analysis of CDT6cc were performed as described (8, 10) with the exception that sedimentation equilibrium scans were carried out at 18,000 rpm.

Xenografting Procedures—The human melanoma cell line BLM and the stable BLM transfectants were xenografted in BALB/C nu/nu mice kept under aseptic conditions, essentially as described (11). Subconflu-

* The costs of publication of this article were defrayed in part by the payment of page charges. This article must therefore be hereby marked "*advertisement*" in accordance with 18 U.S.C. Section 1734 solely to indicate this fact.

§ To whom correspondence should be addressed: Dept. of Molecular Immunology, Netherlands Ophthalmic Research Institute, P. O. Box 12141, 1100 AC Amsterdam, The Netherlands. Tel.: 31-20-5664535; Fax: 31-20-5666121; E-mail: r.peek@ioi.knaw.nl.

[1] The abbreviations used are: CDT6, cornea-derived transcript 6; PBS, phosphate-buffered saline; BrdUrd, bromodeoxyuridine; CMV, cytomegalovirus; RSV, Rous sarcoma virus; MOPS, 4-morpholinepropanesulfonic acid; Tricine, *N*-[2-hydroxy-1,1-bis(hydroxymethyl)ethyl]glycine.

ent cultured cells were detached from the culture flask by treatment with a trypsin/EDTA/glucose solution, washed with phosphate-buffered saline (PBS), and injected subcutaneously into the flanks of mice in a volume of 100 μl of PBS containing 1×10^6 cells. Tumor formation was determined by palpation of the inoculation site. The volume of the subcutaneous tumor was estimated by multiplying length, width, and height of the tumor mass. After obduction, parts of the tumor were snap-frozen and stored in liquid nitrogen. Experiments were performed at least in duplicate, using five mice for each cell line.

Staining of Cultured Cells and Tumor Sections and Analysis of Tumor Vasculature—Blood vessel endothelial cells and extracellular matrix components were stained immunohistochemically by incubation of acetone-fixed 4-μm cryosections with the appropriate antibodies followed by an alkaline phosphatase-labeled secondary antibody. Fixation and immunocytochemical analysis was performed on cultured BLM cells in the same manner as that described for cryosections of xenografts. The VIDAS image analysis system was used to determine number of vessels per surface unit and blood vessel area and diameter (12). Proteoglycans were visualized by conventional Alcian blue or Azan staining. To test the integrity of the vasculature, tumor-bearing mice were injected in the tail vein with monoclonal antibody 9F1 1 and 10 min before sacrificing. Tumor sections were stained directly with a biotin-labeled secondary antibody to visualize endothelial cell-bound 9F1 antibody.

Eukaroytic Expression Constructs and BLM Transfection—The complete open reading frame of CDT6 was cloned in pORSV and pRCMV2 (Invitrogen, Carlsbad, CA). BLM cells were grown to subconfluency and transfected with linearized plasmids using the DOSPER transfection reagent (Roche Molecular Biochemicals).

After 2 days G418 was added to a final concentration of 200 μg/ml, and after 2 weeks cells from G418-resistant foci were isolated and grown separately. Stable expression of CDT6 by individual BLM clones was confirmed by PCR and Northern blot.

Analysis of RNA—Total RNA from cell cultures or from cryosections of tumor tissue was prepared using the RNAzol reagent (Cinna/Biotech Laboratories, Houston, TX) according to the manufacturer's instructions. Ten μg of RNA was size-fractionated on a 1% agarose, 2 M formaldehyde gel in MOPS buffer and blotted to Hybond N filter in 10× SSC after transfer blots were hybridized with random prime-labeled cDNA probes. For reverse transcriptase-PCR analysis, 5 μg of total RNA was reverse-transcribed in the presence of oligo$(dT)_{12-18}$ and 200 units of Superscript Range H reverse transcriptase (Invitrogen) according to the manufacturers' instructions. PCR was performed in a thermocycler (PerkinElmer Life Sciences) for 23 cycles. For amplification of CDT6, the primers 5′-GGACTTCTGGCTGGGGAACG-3′ and 5′-CCAGTAGCCACCTTTGCGGA-3′ were used, and for amplification of β-actin primers 5′-ATGCATTGTTACAGGAAGTCC-3′ and 5′-TACATCTCAAGTTGGGGGAC-3′ were used. Reaction products were size-fractionated on agarose gels.

Western Blot Analysis—Secreted proteins in culture supernatant and total protein extracts of transfected cell lines and controls were obtained by an overnight incubation of subconfluent cultures in medium without fetal calf serum. Culture supernatant was concentrated 10 times with Centricon filter devices (Millipore). Total cell proteins were obtained by extensive washing of the attached cells with PBS followed by lysis in SDS-PAGE sample buffer. Human corneal tissue was obtained from donor eyes that were processed at the Eye Bank of the Netherlands Ophthalmic Research Institute. The corneas used had been donated for transplantation but had been found unacceptable because of changes in the endothelium. To obtain a total corneal protein extract, corneas were first snap-frozen in liquid nitrogen and subsequently homogenized in SDS-PAGE sample buffer using a pestle and a mortar. To aliquots of this corneal extract β-mercaptoethanol was added to a final concentration of 0, 1, 5, 10, or 1000 mM. Proteins were size-fractionated by 10% SDS-PAGE and subsequently electroblotted onto nitrocellulose filters. Blots were incubated with affinity-purified anti-CDT6, washed, and incubated with a goat anti-rabbit peroxidase-conjugated secondary antibody (DAKO, Glostrup, Denmark). Bound antibodies were visualized using a chemiluminescence substrate prepared according to the manufacturer's instructions (ECL; Amersham Biosciences).

Proliferation Assay—BLM cells and stable transfectants were plated at 5,000 cells/well in triplicate flat bottom 96-well dishes in medium without G418. After 1 day BrdUrd was added. For the next 8 days, each day part of the cells were fixed and denatured, and incorporated BrdUrd was quantified immunochemically according to the manufacturer's protocol (Roche Molecular Biochemicals).

Immunoelectron Microscopy of Tissue Samples—Tissue samples were fixed in periodate/lysine/paraformaldehyde for 60 min at room temperature, washed three times with PBS, incubated in 2 M saccharine for cryoprotection, and then snap-frozen in liquid nitrogen. Twenty μM cryosections were preincubated for 30 min with PBS containing 1% bovine serum albumin to reduce background. Sections were stained with 9F1 antibody overnight at 4 °C, washed and incubated with rabbit anti-rat peroxidase-labeled F(ab)2 fragments (Harlan Sera-lab). After staining with diaminobenzidine sections were washed with water and postfixed for 15 min with 1% osmium tetroxide. Ultrathin sections were stained with uranyl acetate and examined with a JEOL 1200 EX/II electron microscope at 50 kV.

RESULTS

CDT6 Is a Secreted Protein Expressed in the Stromal Layer of the Human Cornea—We have shown recently (4) that CDT6 expression is restricted to the stromal layer of the human cornea. To analyze the expression of CDT6 on the protein level, a polyclonal antibody was raised against the predicted coiled-coil domain of CDT6 (Glu-47 to Glu-122), which has no significant sequence similarity to known angiopoietins. Western blot analysis of a total protein extract from human cornea with this antibody detected a single, slightly larger band of 45 kDa than expected for CDT6 with a molecular mass of 38 kDa. This indicated that the protein may be produced in a glycosylated form (Fig. 1*a*).

Immunohistochemical analysis of cryosections of human cornea with the anti-CDT6 antibody revealed a thread-like staining of the stromal layer. Staining was also observed for the junction between the corneal stromal layer and the conjuctiva, whereas the sclera was negative for CDT6 expression (Fig. 1*b*).

To demonstrate that CDT6 is a secreted protein, a human melanoma cell line BLM (13) was stably transfected with a mammalian expression vector containing the CDT6 open reading frame under the control of the cytomegalovirus (CMV) immediate-early promoter. Analysis of the culture supernatant and cell lysates of these tranfectants showed that CDT6 was readily detectable in the supernatant and weakly in the cell lysate (Fig. 1*c*). This finding demonstrates that the signal sequence of CDT6 is functional, resulting in the secretion of the protein.

CDT6 Forms a Disulfide-linked Homotetramer Assembled by Coiled-coil α-Helices—Secondary structure analysis of the CDT6 protein, using the COILS algorithm (version 2.2) (14, 15), which compares an amino acid sequence with sequences in a data base of known two-stranded coiled coils, predicted with high probability a coiled-coil stretch from amino acid residues Glu-47 to Gln-122. For other regions of the sequence, a tendency to assume a coiled-coil conformation was not predicted. To confirm the presence of a coiled-coil domain in CDT6, a recombinant polypeptide chain (termed CDT6cc) that corresponds to the predicted sequence stretch was produced by heterologous gene expression in *Escherichia coli.* The homogeneity of affinity-purified CDT6cc was assessed by Tricine/SDS-PAGE. A single band migrating with a mobility corresponding to its expected molecular mass was detected (not shown).

CD spectroscopy was used to test for the secondary structure of the recombinant protein. The far-ultraviolet CD spectrum recorded from CDT6cc at 5 °C was characteristic of an α-helical structure with minima near 208 and 222 nm (Fig. 2*A*). A $[\theta]_{222}$ value of $-37{,}000$ degree cm^2 dmol^{-1} indicated a degree of α-helicity of ~100% for a 29 μM total protein solution (10).

The stability of the recombinant protein was assessed by a temperature-induced CD unfolding profile recorded at 221 nm. The thermal unfolding profile exhibited the sigmoid shape typical for coiled coils, implying a two-state transition. Accordingly, the profile was monophasic and reversible with >90% of the starting signal regained upon cooling. At a total protein

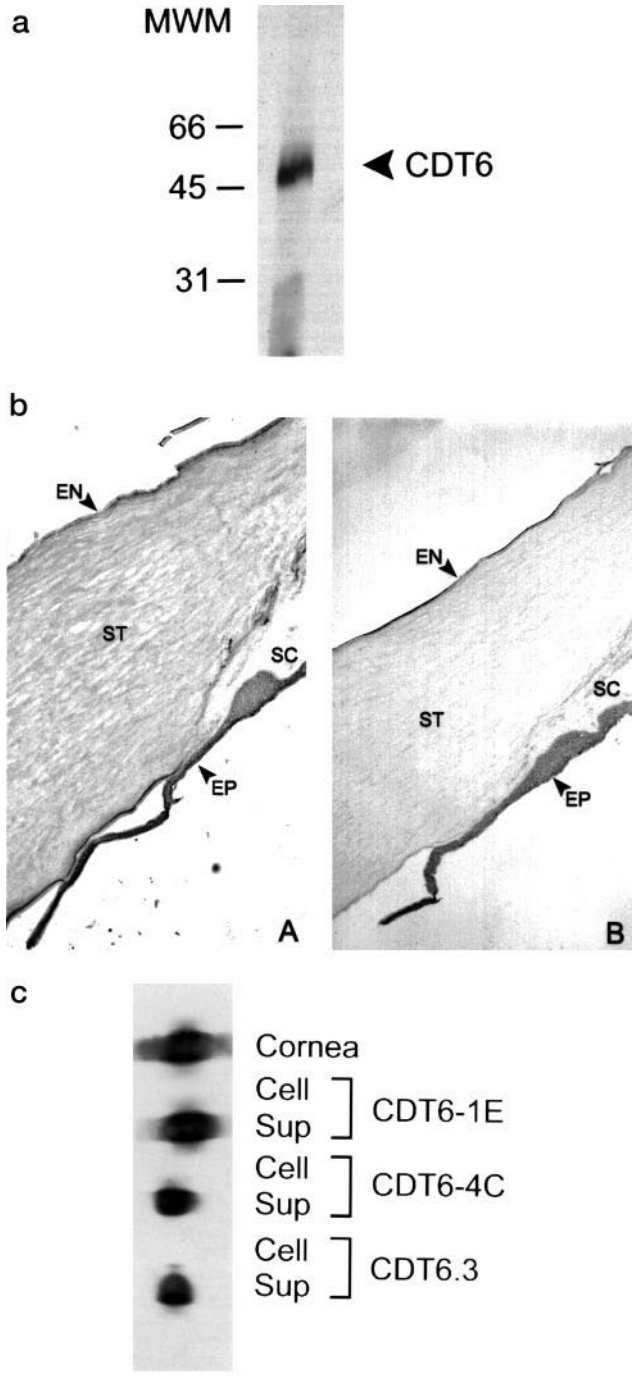

FIG. 1. **CDT6 is a secreted 45-kDa protein expressed in the stromal layer of the human cornea.** *a*, Western blot analysis of a human corneal extract with an affinity-purified anti-CDT6 antibody, molecular weight markers (*MWM*) are indicated. *b*, tissue sections of human cornea stained with anti-CDT6 antibody (*A*) and a control antibody (*B*). *EN,* endothelial cell layer; *ST*, stromal layer; *EP*, epithelium; *SC*, sclera. It should be noted that the epithelial layer was partially detached from the cornea during preparation of the sections. *c*, cell culture media and cell lysates of stably transfected BLM cell lines were analyzed by Western blot using anti-CDT6 antibody. *Sup*, supernatant; *Cell*, cell lysate.

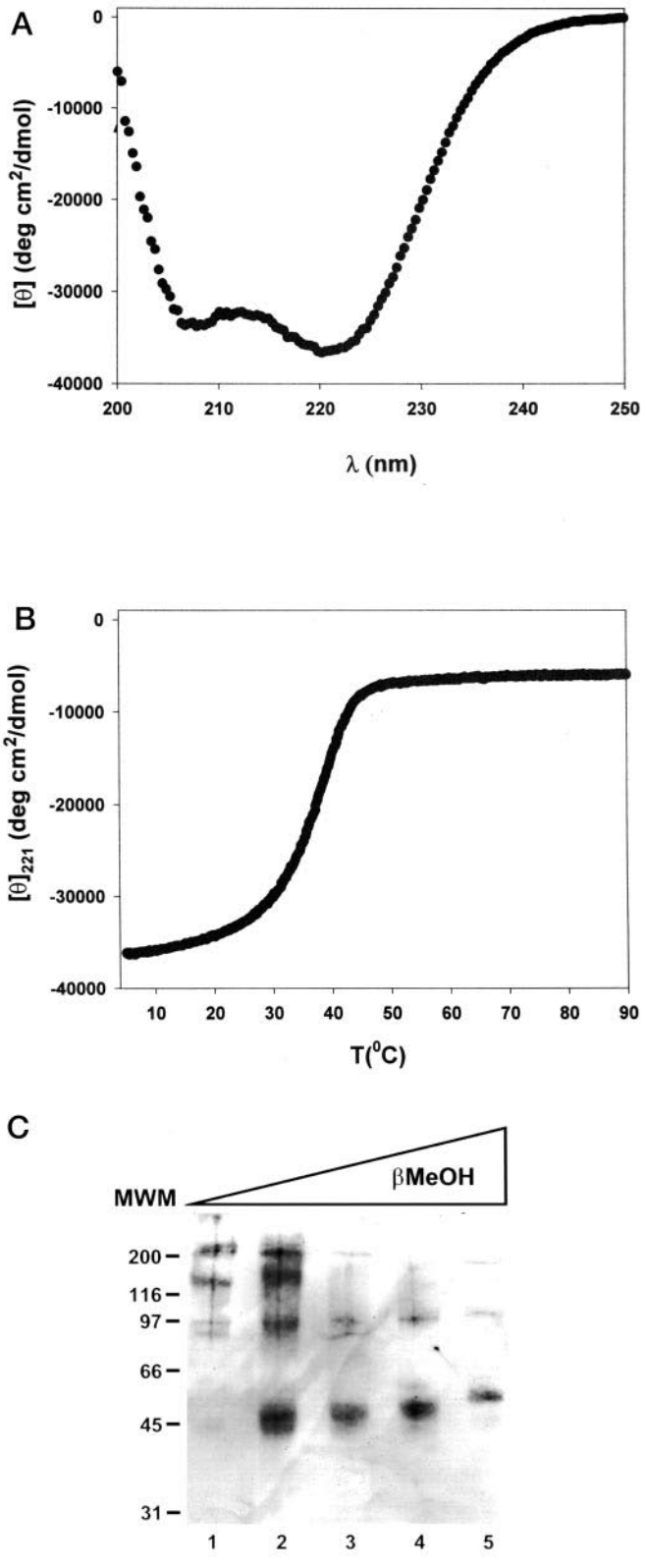

FIG. 2. **CDT6 is a disulfide-linked, four-stranded coiled-coil protein.** *A*, far-UV CD spectrum recorded at 5 °C, and *B*, temperature-induced unfolding profile of recombinant CDT6cc. Thermal stability of the peptide was monitored by the change of the CD signal at 222 nm. The polypeptide chain concentration was 29 μM in 5 mM sodium phosphate buffer (pH 7.4) containing 150 mM sodium chloride. *C*, total protein extract of human cornea treated with increasing amounts of β-mercaptoethanol (β*MeOH*) was assayed by Western blot analysis using the anti-CDT6 antibody. *Lane 1*, 0 mM; *lane 2*, 1 mM; *lane 3*, 5 mM; *lane 4*, 10 mM; *lane 5*, 1000 mM. The positions of the molecular weight markers are indicated (*MWM*).

concentration of 29 μM, the profile showed a T_m at about 37 °C (Fig. 2*B*).

To determine the oligomerization state of CDT6cc, the polypeptide chain fragment was analyzed by analytical ultracentrifugation. Sedimentation equilibrium yielded a molecular mass of 34.9 ± 2.6 kDa at 20 °C. This value is consistent with the formation of a tetramer (calculated molecular mass of 35.6

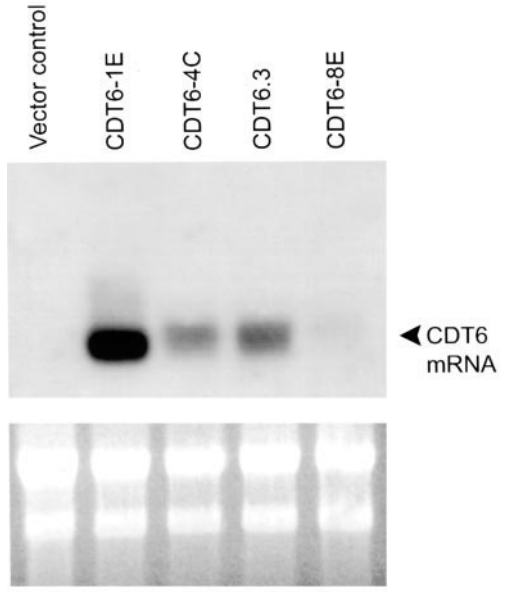

FIG. 3. **Northern blot analysis of BLM cell lines stably transfected with CDT6 expression constructs or controls.** Each lane contains ~10 μg of total RNA. Hybridization was performed with a probe that spans the entire CDT6 coding sequence. As a control for the amount and integrity of the RNA, ethidium bromide-stained ribosomal RNA is shown at the *bottom.*

kDa). Sedimentation velocity revealed a sedimentation coefficient of 2 S.

The oligomerization state of native CDT6 was determined by Western blot analysis of a protein extract of human cornea that was treated with increasing amounts of a reducing agent. Under non-reducing conditions, the affinity-purified antibody against CDT6 detected bands around 150 and 200 kDa (Fig. 2*C*, *lane 1*). Addition of β-mercaptoethanol to 1 mM resulted in the appearance of a band around 90 kDa and several bands around 45 kDa. At higher concentrations of β-mercaptoethanol the high molecular bands disappeared, and the multiple bands at 45 kDa were reduced to a single band (Fig. 2*C*, *lane 5*). The bands at 90, 150, and 200 kDa most likely represent CDT6 dimers, trimers, and tetramers, respectively. The multiple bands at 45 kDa probably result from partial reduction of intramolecular disulfide bridges within the fibrinogen-like domain, leading to a gradual unfolding of this globular structure. These results indicate that *in vivo* CDT6 exists predominantly as disulfide-linked homotrimers and homotetramers.

CDT6 Expression Inhibits Tumor Growth in Xenotransplanted Nude Mice—To determine the function of CDT6 *in vivo*, a human melanoma cell line (BLM) was used. The biological behavior of this melanoma cell line after xenografting into nude mice has been studied in detail (11, 16). The cell line was obtained from a surgically removed lymph node metastasis (13). BLM cells are well suited to study the effect of a protein on a growing tissue *in vivo* because they produce highly vascularized tumors within 1 month after subcutaneous inoculation. To induce CDT6 expression, BLM cells were stably transfected with mammalian expression vectors in which CDT6 expression was driven by either the Rous sarcoma virus early gene promoter (RSV-CDT6 constructs) or by the cytomegalovirus immediate-early promoter (CMV-CDT6 constructs). Transfected BLM cell lines were analyzed for CDT6 expression by Northern blot (Fig. 3) and semi-quantitative PCR (not shown). From the RSV-CDT6 transfectants, a cell line with intermediate (RSV.CDT6.9) and high level expression (RSV.CDT6.3) was selected. In the vector control, the CDT6 open reading frame was replaced by the chloramphenicol acetyltransferase coding sequence. From the CMV-CDT6 transfectants, three cell lines were selected as follows: CMV.CDT6–8E (low expression), CDT6–4C (intermediate expression), and CDT6–1E (high expression).

To assay the effect of CDT6 expression on BLM cell growth *in vitro*, all cell lines were tested in a proliferation assay. Proliferation curves did not show a significant effect of CDT6 on *in vitro* growth of the CDT6 transfectants as compared with the vector control or the parental BLM cell line (Fig. 4*a*).

To study the role of CDT6 *in vivo,* all cell lines were injected subcutaneously in the flanks of nude mice. Primary tumor formation and xenograft growth were monitored for 4 weeks. Although all cell lines gave rise to tumors within 1 week after inoculation, the growth characteristics of the various BLM transfectants appeared to be markedly different from those of the controls. In line with previous studies (11, 16, 17), the parental cell line and the vector controls grew to tumors exceeding a volume of 2.5 cm^3 within 4 weeks after tumor induction. In contrast, the RSV-CDT6 transfectants were about 6-fold smaller than the controls 4 weeks after tumor induction (Fig. 4, *b* and *c*). Also the CMV-CDT6 transfectants grew considerably slower than the controls. Interestingly, growth rates of the CMV-CDT6 transfectants appeared to be correlated with CDT6 expression. The growth curve for cell line CMV-CDT6.8E with the lowest CDT6 expression was very similar to that of the parental BLM line, whereas CDT6.1E with high level CDT6 expression showed the slowest tumor growth (Fig. 4*b*). Reverse transcriptase-PCR analysis of control and CDT6 tumors showed that CDT6 mRNA expression could still be readily detected in end-stage (4 weeks) tumors (Fig. 4*d*).

Histological Analysis of Xenografts Expressing CDT6—At various times after tumor induction, mice were sacrificed, and tumors were surgically removed. Remarkably, tumor tissue of xenografts expressing CDT6 was more solid compared with control tumors (results not shown). To determine which process was responsible for the impaired growth of xenografts by CDT6, tumors were analyzed by histological and immunohistological techniques. Angiopoietins are known to act mainly on vascular endothelium by angiogenic remodeling and vessel maturation and stabilization. To determine the effect of CDT6 on blood vessel formation, tumor sections were stained with a rat monoclonal antibody (9F1) (11), which highlights mouse blood vessel endothelial cells. As shown in Fig. 5*A*, blood vessels in tumors expressing CDT6 were abnormally shaped and displayed an aberrant tortuous morphology with endothelial cell protrusions extending between tumor cells. Automated image analysis revealed that the number of blood vessel sprouts appeared to be reduced in CDT6 tumors, whereas vessel diameter and surface of the lumen were significantly increased in these tumors (Fig. 6). Blood flow and vessel wall integrity was confirmed by intravenous injection of the 9F1 anti-endothelial cell monoclonal antibody in the tail of living mice bearing control or CDT6 tumors. In all tumors anti-9F1 staining was observed only on the luminal side of blood vessels, without detectable leakage of the antibody in the surrounding tissue (data not shown).

CDT6 Expression Induces Deposition of Corneal Stromal Layer Typical of Extracellular Matrix Components in Xenografts—Several lines of evidence indicated that CDT6 expression did influence the structure of the extracellular matrix. First, tumor tissue of xenografts expressing CDT6 were more solid as compared with control tumors. Second, as shown in Fig. 5*B*, cells also appeared to align to higher order structures leading to a turbulent morphology. To address this matter, sections of tumor tissue were stained immunohistochemically for various matrix components, including laminin, fibronectin,

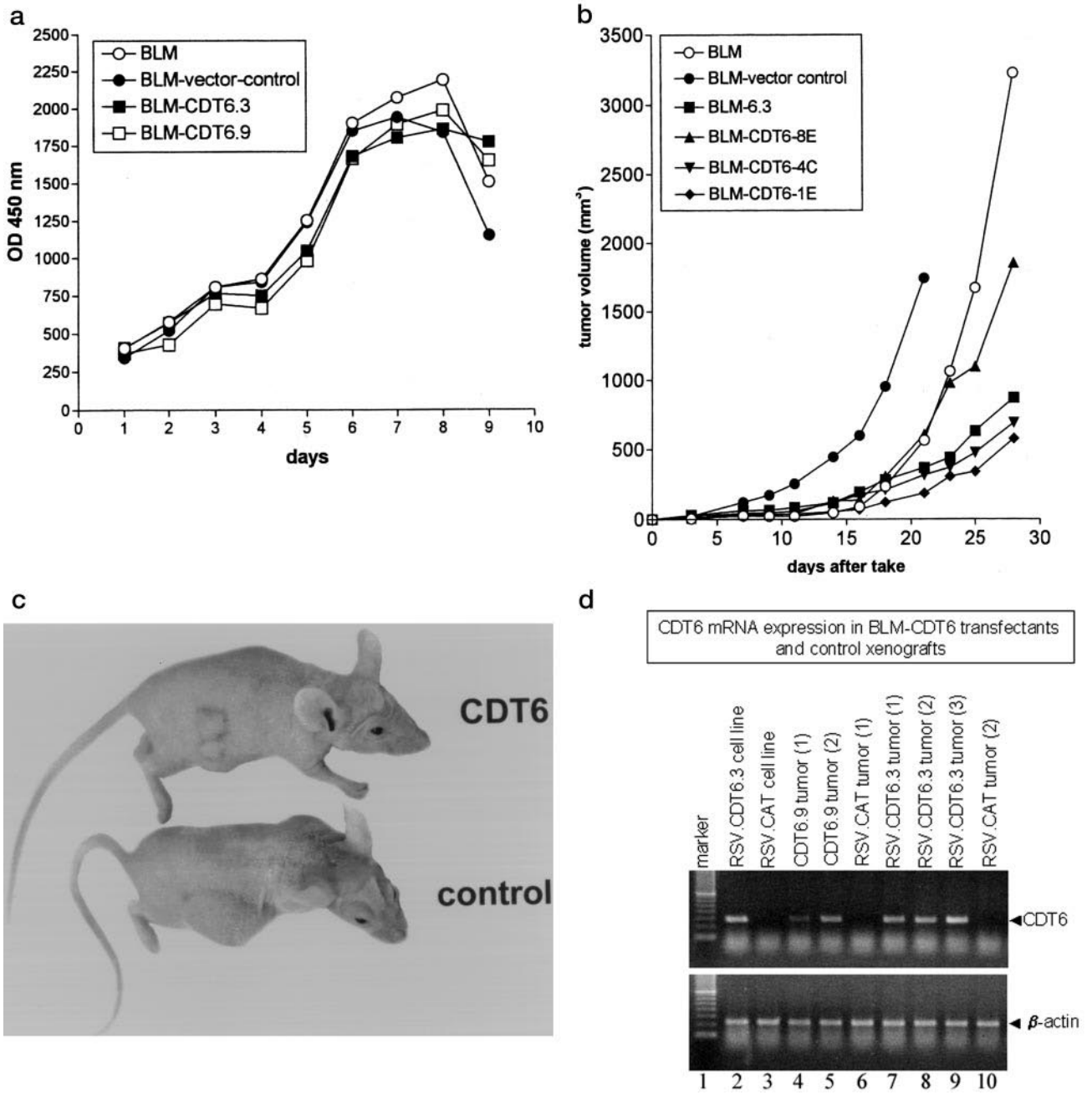

FIG. 4. **CDT6 expression inhibits tumor growth in xenotransplanted nude mice.** *In vitro* and *in vivo* proliferation of BLM cells stably transfected with CDT6 and controls. *a*, cells were seeded at 5000 cells cm^2, and proliferation was measured at 9 subsequent days in a BrdUrd incorporation assay (for technical details see "Experimental Procedures"). *b*, growth curves of subcutaneous *in vivo* xenografts obtained from a RSV-CDT6 transfectant and CMV-CDT6 transfectant. Each point represents the mean volume of five xenografts. The volume of the xenografts was measured every 2nd day. *Error bars* were omitted for reasons of clarity but were generally less than 40%. *c*, appearance of mice with xenografts 4 weeks after tumor induction. *d*, reverse transcriptase-PCR analysis of CDT6 expression in end stage (4 weeks) BLM-CDT6-transfected and control xenografts (*lanes 4–10*). A BLM-CDT6 cell line and a vector control cell line were also analyzed (*lanes 2* and *3*). The *bottom panel* shows the control PCR for β-actin expression.

collagen I, IV, and V. Additionally, proteoglycans were stained using Alcian blue and Azan staining. In Fig. 5 results from these stainings are shown for 4-week-old tumors. Analysis performed on tumors from earlier time points showed similar results (data not shown). Notably, the amounts of collagen types I and V and proteoglycans were increased in CDT6-expressing tumors. In *in vitro* studies, cultured control and CDT6-expressing tumor cells from clone BLM CDT6.1E were stained for collagen I and V as well. Expression of both extracellular matrix components was clearly increased in the transfected tumor cells (Fig. 7). In contrast, no difference was observed for the expression of laminin, fibronectin, and collagen IV between CDT6 tumors and controls. Control tumors showed a patchy distribution of collagen types I and V with the highest expression around blood vessels. In contrast, in tumors expressing CDT6, collagen I and V formed long thread-like structures that were not confined to the tissue surrounding the blood vessels but extended throughout the tumor. These structures closely resembled the turbulent pattern of the tumor cell mass (Fig. 5, *C* and *D*). These findings were confirmed by a

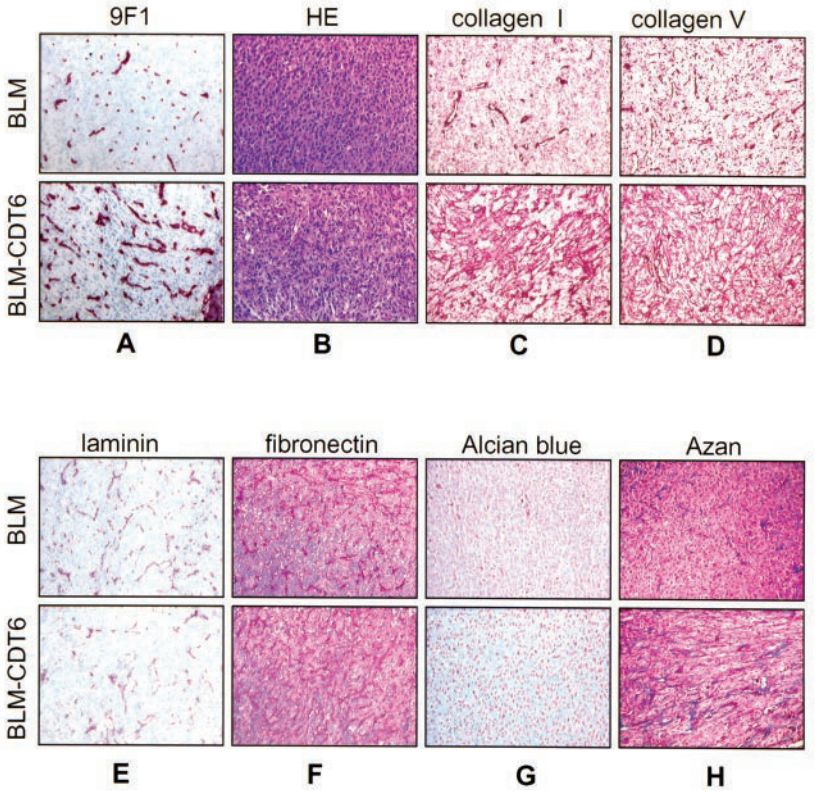

FIG. 5. **CDT6 expression induces deposition of extracellular matrix components in xenografts.** Histochemical analysis of tissue sections of xenografts of CDT6 transfectants and controls stained with rat anti-mouse endothelial cell monoclonal antibody 9F1 (*A*), hematoxylin (*B*), anti-collagen I (*C*), anti-collagen V (*D*), anti-laminin (*E*), anti-fibronectin (*F*), and with Alcian blue and Azan for proteoglycans (*G* and *H*). All sections were weakly hematoxylin-counterstained.

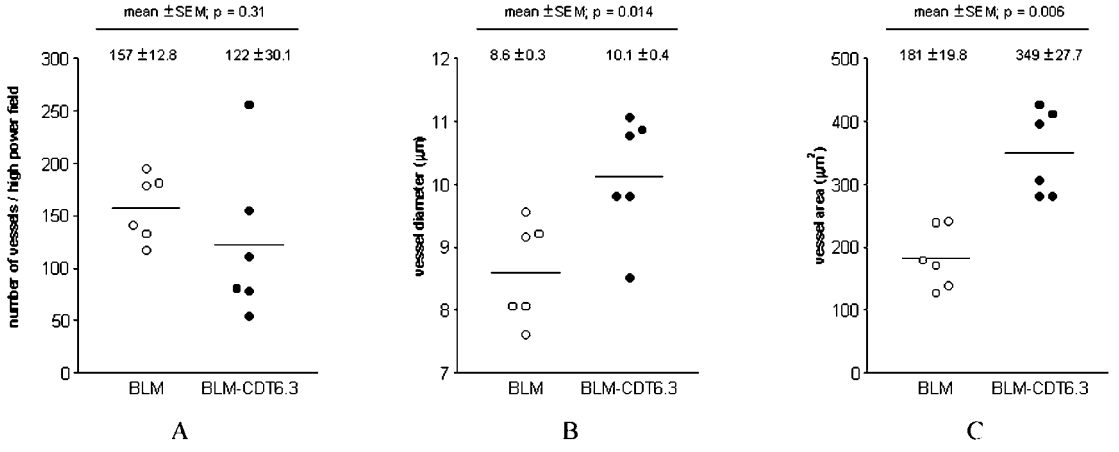

FIG. 6. **The effect of CDT6 on tumor angiogenesis.** Density (*A*), diameter (*B*), and surface (*C*) of blood vessels of CDT6 xenografts and controls, as determined by automated image analysis. *Each circle* represents a xenograft of RSV-CDT6.3-transfected cells (●) and the RSV-chloramphenicol acetyltransferase vector control (○).

detailed electron microscopy analysis tumor sections stained with the monoclonal antibody against mouse blood vessel endothelial cells. Electron microscopy revealed large deposits of collagen fibrils in the extracellular space surrounding the blood vessels in tumors expressing CDT6 (Fig. 8).

DISCUSSION

Several angiopoietins and angiopoietin-like proteins molecules have recently been identified (5–7, 18–20). "True" angiopoietins differ from angiopoietin-like proteins by their ability to bind to the largely endothelial-specific Tie2 receptor. As angiopoietin-like proteins, like angiopoietins, effect angiogenesis, they must use different mechanisms of signal transduction. In this report, we describe the structural and functional characterization of the human corneal angiopoietin-like factor CDT6. We found that CDT6 is produced as a secreted protein with an apparent molecular mass of 45 kDa. The fact that the molecular mass of CDT6 was larger than the expected molecular mass of 38 kDa, as calculated from its amino acid sequence, indicates post-translational modification of the protein. Consistent with this observation, the open reading frame of CDT6 contains several potential *N*-glycosylation sites (4). This suggests that CDT6, similar to the angiopoietins, is produced as a glycoprotein.

In angiopoietins, the coiled-coil domain mediates the formation of homo-oligomers that are stabilized by interchain disulfide bridges (7, 21, 22). This results in clustering of the globular fibrinogen-like domains. This is thought to be required for the interaction of angiopoietins with the Tie2 receptor and thus might be crucial for ligand-mediated activity of the Tie receptor. By using CD spectroscopy and analytical centrifugation, we demonstrated that the predicted coiled-coil segment of CDT6 folds into a tetrameric coiled-coil structure *in vitro*. Consistent

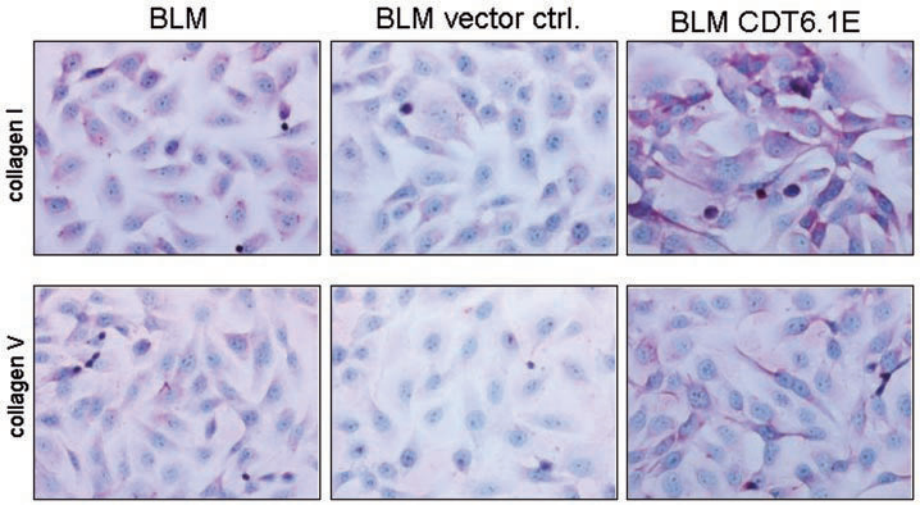

FIG. 7. **Immunocytochemical analysis of control and CDT6-expressing tumor cells.** BLM cells, BLM-CDT6.1E, and vector-transfected control cells were stained with anti-collagen I and anti-collagen V. Cells were weakly hematoxylin-counterstained.

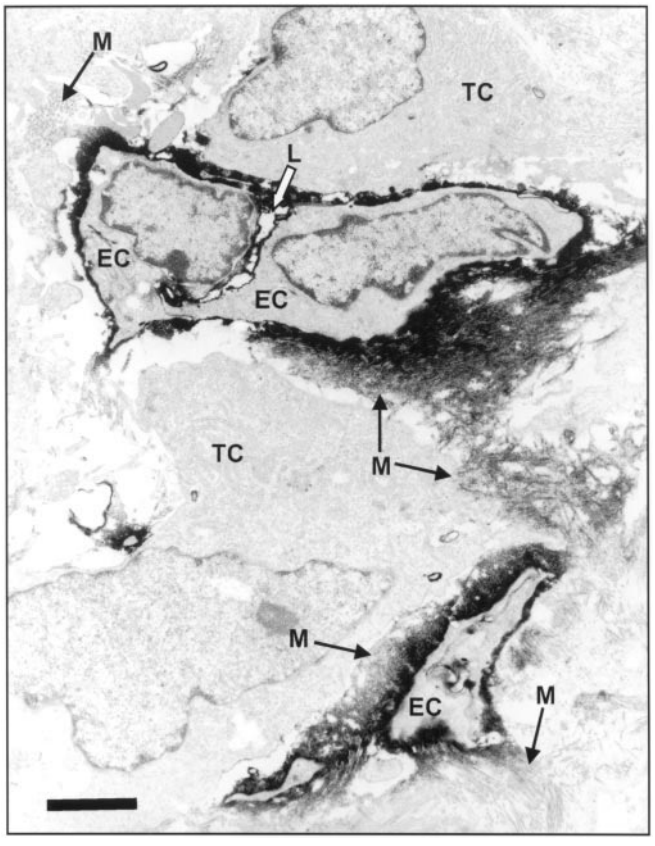

FIG. 8. **Electron microscopy of an RSV-CDT6 xenograft stained with monoclonal antibody 9F1.** *EC*, blood vessel endothelial cell; *L*, blood vessel lumen; *TC*, BLM tumor cells; *M*, extracellular matrix deposits oriented in various directions. *Bar* indicates 2 μm.

with these findings, CDT6 *in vivo* exists predominantly as disulfide-linked homotrimers and homotetramers. The intermolecular disulfide bridges are most likely formed by cysteine residues that flank the coiled-coil domain. These findings suggest that clustering of the fibrinogen-like domains of CDT6 might be required for the interaction of the protein with a yet unknown receptor on the cell surface.

By expressing CDT6 in a human xenograft model, we demonstrated that this protein has a dramatic effect on a growing tissue with a high vascular density. Interestingly, in xenografts with the highest expression of CDT6, tumor volume was reduced up to 6-fold 4 weeks after inoculation. As these tumors require a dense vascular network for rapid growth the expression of CDT6, similar to that of angiopoietins, might interfere with angiogenesis resulting in a suppression of tumor growth. Consistent with this assumption, immunohistochemical analysis of tissue sections of CDT6 expressing xenografts stained for blood vessel endothelial cells indeed showed aberrant blood vessels. The blood vessel diameter and lumen was significantly increased as determined by automated image analysis (12). From these results we initially assumed that similar to angiopoietin-1 and angiopoietin-2, CDT6 was involved in vascular morphogenesis. However, not only blood vessel endothelial cells but also the tumor cells themselves appeared to be affected in their morphology by expressing CDT6. Whereas the cells in control tumors were spaced in a relatively ordered fashion, in the CDT6 tumors cells were more elongated and appeared to align to higher order structures.

In theory, the observed increase in extracellular matrix components might also be accounted for by a CDT6-induced fibrotic response of host (mouse) cells such as fibroblasts as a defense against the invading tumor cells. For several reasons, however, we think that the extracellular matrix production is tumor cell-derived rather than host cell-derived. First, fibrotic tissue consists mainly of fibronectin, laminin, and collagen types I, III, and IV (23–26). Collagen type V was hardly ever observed in fibrotic tissue (27–28), whereas we found an abundant increase in expression of collagen V in CDT6-expressing tumors. In contrast, an increase in expression of fibronectin, collagen IV, and laminin was not observed (Fig. 5). Second, staining for extracellular matrix components in general (Azan and Alcian blue, Fig. 5) showed individual tumor cells surrounded by large amounts of ECM. This strongly suggests that the CDT6-expressing tumor cells, rather than host cells (endothelial cells and fibroblasts), produce the large amount of ECM. Finally, staining for collagen types I and V on cultured control and CDT6 transfected tumor cells showed an increased expression of these collagen types by CDT6 transfectants.

In addition to the CDT6-expressing tumor cells it appeared also that the blood vessel endothelial cells contributed to the increase in the extracellular matrix components, as evidenced by microscopic analyses. Increased deposition of these extracellular matrix components results not only in aberrant tumor morphology but is probably also responsible for the abnormal morphology seen for the blood vessels. As angiogenesis involves breakdown of the extracellular matrix before endothelial cells can migrate, the dense and more rigid extracellular matrix of CDT6 tumors might partially block this process leading to abnormally formed blood vessels. Possibly these abnormal blood vessels do not supply the surrounding tumor tissue with

oxygen and nutrients as efficient as in controls resulting in impaired tumor growth. Alternatively, the extracellular matrix in CDT6 tumors might allow diffusion of nutrients less efficiently also leading to a reduction in tumor growth.

The CDT6-induced drastic increase in the production of distinct extracellular matrix components indicates that this protein has an important function in the human cornea. With its characteristic uniform diameter of striated collagen fibrils in the stromal layer, the cornea has the highest collagen V content of all human tissues and contains up to 5-fold more type V collagen than those of tendon and sclera. The interaction between type I and type V collagen regulates fibril diameter, whereas the interactions between collagens and proteoglycans define the spacing of these fibrils. Both processes are thought to be crucial for optical transparency (29–31). Thus, the increased production of collagen I and V and proteoglycans but not other extracellular matrix components in CDT6-expressing tumors mimics the natural situation in the cornea stromal layer. Consistent with this notion, tissue sections of these tumors resemble highly disorganized stromal layers in which the tumor cells are stretched in a similar manner as the cornea stromal keratocytes. These observations suggest that CDT6 functions as a morphogen, which induces differentiation toward a corneal keratocyte phenotype. CDT6 may exert this function on corneal keratocytes *in vivo* through an autocrine mechanism to compensate for loss of extracellular matrix components by protein turnover and to restore corneal integrity in case of tissue damage.

Recently, CDT6 was independently cloned from human ovary (7). Together with our xenograft results, these findings indicate that the receptor for CDT6 is not cell type-specific. The fact that we were not able to demonstrate significant CDT6 expression in other human tissues (4) suggests that high level expression of CDT6 is restricted to the cornea stromal layer. This assumption is consistent with our findings that high level expression of CDT6 had a much stronger impact on tumor morphology than low level expression. However, the observation that CDT6 is also expressed in other tissues suggests additional possible functions for this protein.

Acknowledgments—We thank R. van't Hullenaar, B. Heijdra, L. Broersma, and B. Meek for technical assistance.

REFERENCES

1. Klyce, S. D., and Beuerman, R. W. (1988) in *The Cornea* (Kaufmann, H. E., Barron, B. A., McDonald, M. B., and Waltman, S. R., eds) pp. 3–54, Churchill Livingstone, New York
2. Fujimaki, T., Hotta, Y., Sakuma, H., Fujiki, K., and Kanai, A. (1999) *Cornea* **18,** 109–114
3. Nishida, K., Adachi, W., Shimizu-Matsumoto, A., Kinoshita, S., Mizuno, K., Matsubara, K., and Okubo, K. (1996) *Invest. Ophthalmol. Vis. Sci.* **37,** 1800–1809
4. Peek, R., van Gelderen, B. E., Bruinenberg, M., and Kijlstra, A. (1998) *Invest. Ophthalmol. Vis. Sci.* **39,** 1782–1788
5. Davis, S., Aldrich, T. H., Jones, P. F., Acheson, A., Compton, D. L., Jain, V., Ryan, T. E., Bruno, J., Radziejewski, C., Maisonpierre, P. C., and Yancopoulos, G. D. (1996) *Cell* **27,** 1161–1169
6. Maisonpierre, P. C., Suri, C., Jones, P. F., Bartunkova, S., Wiegand, S. J., Radziejewski, C., Compton, D., McClain, J., Aldrich, T. H., Papadopoulos, N., Daly, T. J., Davis, S., Sato, T. N., and Yancopoulos, G. D. (1997) *Science* **277,** 55–60
7. Valenzuela, D. M., Griffiths, J. A., Rojas, J., Aldrich, T. H., Jones, P. F., Zhou, H., McClain, J., Copeland, N. G., Gilbert, D. J., Jenkins, N. A., Huang, T., Papadopoulos, N., Maisonpierre, P. C., Davis, S., and Yancopoulos, G. D. (1999) *Proc. Natl. Acad. Sci. U. S. A.* **96,** 1904–1909
8. Kammerer, R. A., Schulthess, T., Landwehr, R., Lustig, A., Fischer, D., and Engel, J. (1998) *J. Biol. Chem.* **273,** 10602–10608
9. Edelhoch, H. (1967) *Biochemistry* **6,** 1948–1954
10. Chen, Y. H., Yang, J. T., and Chau, K. H. (1974) *Biochemistry* **30,** 3350–3359
11. Westphal, J. R., van't Hullenaar, R. G., van der Laak, J. A., Cornelissen, I. M., Schalkwijk, L. J., van Muijen, G. N., Wesseling, P., de Wilde, P. C., Ruiter, D. J., and de Waal, R. M. (1997) *Br. J. Cancer* **76,** 561–570
12. Van der Laak, J. A., Westphal, J. R., Schalkwijk, L. J., Pahlplatz, M. M., Ruiter, D. J., de Waal, R. M., and de Wilde, P. C. (1998) *J. Pathol.* **184,** 136–143
13. Van Muijen, G. N., Cornelissen, L. M., Jansen, C. F., Figdor, C. G., Johnson, J. P., Brocker, E. B., and Ruiter, D. J. (1991) *Clin. Exp. Metastasis* **9,** 259–272
14. Lupas, A. (1996) *Trends Biochem. Sci.* **21,** 375–382
15. Lupas, A. (1996) *Methods Enzymol.* **266,** 513–525
16. Van Muijen, G. N., Jansen, K. F., Cornelissen, I. M., Smeets, D. F., Beck, J. L., and Ruiter, D. J. (1991) *Int. J. Cancer* **48,** 85–91
17. Westphal, J. R., Van't Hullenaar, R., Peek, R., Willems, R. W., Crickard, K., Crickard, U., Askaa, J., Clemmensen, I., Ruiter, D. J., and De Waal, R. M. (2000) *Int. J. Cancer* **86,** 768–776
18. Kim, I., Moon, S. O., Koh, K. N., Kim, H., Uhm, C. S., Kwak, H. J., Kim, N. G., and Koh, G. Y. (1999) *J. Biol. Chem.* **274,** 26523–26528
19. Kim, I., Kwak, H. J., Ahn, J. E., So, J. N., Liu, M., Koh, K. N., and Koh, G. Y. (1999) *FEBS Lett.* **443,** 353–356
20. Conklin, D., Gilbertson, D., Taft, D. W., Maurer, M. F., Whitmore, T. E., Smith, D. L., Walker, K. M., Chen, L. H., Wattler, S., Nehls, M., and Lewis, K. B. (1999) *Genomics* **62,** 477–482
21. Procopio, W. N., Pelavin, P. I., Lee, W. M., and Yeilding, N. M. (1999) *J. Biol. Chem.* **274,** 30196–30201
22. Kim, I., Kim, J. H., Ryu, Y. S., Jung, S. H., Nah, J. J., and Koh, G. Y. (2000) *J. Biol. Chem.* **275,** 18550–18556
23. Paczek, L., Bartlomiejczyk, I., Gradowska, L., Szmidt, J., Rowinski, W., Gaciong, Z., Heidland, A., and Laskowska-Klita, T. (1996) *Ann. Transplant.* **1,** 41–43
24. Magro, G., Fraggetta, M. G., Travalis, S., and Lanzafame, S. (1997) *Gen. Diagn. Pathol.* **143,** 203–208
25. Mindan, P. F. J., Panzo, A., Lozano, M. D., Herreros, J., and Mejia, S. (1997) *Clin. Transplant.* **11,** 426–431
26. Aycock, R. S., and Seyer, J. M. (1989) *Connect. Tissue Res.* **23,** 19–31
27. Madri, J. A., and Furthmayr, H. (1980) *Hum. Pathol.* **11,** 353–366
28. Vleming, L. J., Baelde, J. J., Westendorp, R. G., Daha, M. R., van Es, L. A., and Bruijn, J. A. (1995) *Clin. Nephrol.* **44,** 211–219
29. McLaughlin, J. S., Linsenmayer, T. F., and Birk, D. E. (1989) *J. Cell Sci.* **94,** 371–379
30. Birk, D. E., Fitch, J. M., Babiarz, J. P., Doane, K. J., and Linsenmayer, T. F. (1990) *J. Cell Sci.* **95,** 649–657
31. Scott, J. E. (1992) *J. Anat.* **180,** 155–164